Solvent-Acidity-Driven Change in Photophysics and Significant Efficiency Improvement in Dye-Sensitized Solar Cells of a Benzothiazole-Derived Organic Sensitizer

Kostas Seintis,[a] *Çiğdem Şahin,*[b,c] *Ivica Sigmundová,*[d] *Elias Stathatos,*[c]

Peter Hrobárik,[e,*] *Mihalis Fakis*[a,*]

[a] Department of Physics, University of Patras, GR-26504, Patras, Greece.

[b] Department of Chemistry, Art & Science Faculty, Pamukkale University, TR-20160 Denizli, Turkey.

[c] Nanotechnology and Advanced Materials Laboratory, Electrical Engineering Department, Technological-Educational Institute of Western Greece, GR-26334 Patras, Greece.

[d] Department of Organic Chemistry, Faculty of Natural Sciences, Comenius University, Mlynská dolina CH-2, Ilkovičova 6, SK-84215 Bratislava, Slovakia.

[e] Department of Inorganic Chemistry, Faculty of Natural Sciences, Comenius University, Mlynská dolina CH-2, Ilkovičova 6, SK-84215 Bratislava, Slovakia.

ABSTRACT. The photophysics and solar cells efficiency of organic sensitizers comprising a cyanoacrylic acid group are greatly influenced by an equilibrium between the neutral (”non-deprotonated”, COOH) and anionic (“deprotonated”, COO^-) forms, whose ratio depends on the solvent polarity and its H-bonding properties, dye concentration and temperature used. Herein, we report a detailed investigation on the relationship between the portions of COOH and COO^- dye forms and the photophysical and solar cell properties of an organic dipolar sensitizer, **BTZA-II**, bearing triphenylamine electron-donating and benzothiazole electron-withdrawing moieties. The photophysics has been studied by stationary and time-resolved fluorescence spectroscopy in apolar and polar solvents with a dye concentration ranging from 5×10^{-7} M to 5×10^{-5} M, also upon addition of small amounts of an external acid or base in order to change the solvent acidity, allowing us to distinguish the contribution and lifetime of the neutral and anionic form. The fluorescence of **BTZA-II** in apolar toluene originates from the neutral form, which has a lifetime of 1.9 ns. Addition of a strong base (1,8-diazabicyclo[5.4.0]undec-7-ene, DBU) shifts the equilibrium towards the less fluorescent anionic COO^- form with a lifetime of 1.1 ns. The situation is different in the polar acetonitrile, where the fluorescence of the anionic form dominates (with a lifetime of 2.0 ns). Adding small amounts of acetic acid (AcOH) protonates the COO^- form of the **BTZA-II** dye and reveals significant quenching of the fluorescence because of the increased contribution of the neutral species with a lifetime of 0.4-0.5 ns. This quenching of the neutral species in acetonitrile has been also observed in concentrated solutions and is due to excited state proton transfer. By contrast, the photophysics of a dye **Btz-NPh2**, similar to **BTZA-II** but without the cyanoacrylic acid group, is not affected upon adding acetic acid (H-donor) or DBU base (H-acceptor), that rules out the Brønsted-base role of the benzothiazole scaffold in the aforementioned observations. Finally, dye-sensitized solar cells (DSSCs) with a solid-state electrolyte were prepared from toluene and toluene+acid solutions. A significant increase of the solar cell efficiency, η, by 58% (η reaching a value of 4.9%) has been achieved after addition of a small, appropriate amount of acetic acid into the initial **BTZA-II** dye solution.

INTRODUCTION

Organic dyes used as sensitizers in Dye Sensitized Solar Cells (DSSCs) have gained tremendous scientific attention since they exhibit low production costs, high molar extinction coefficients and a large variety of structural modifications, which allow a specific tailoring of their properties at the molecular level to meet all the application requirements.[1-18] Typically, organic sensitizers consist of an electron donating group, a π-conjugated bridge and an electron accepting unit.[19-33] In addition, an anchoring group (usually comprising a carboxylic acid moiety, COOH) is introduced, that allows the chemical adsorption of the dye on the metal-oxide semiconductor. The most important process after light harvesting by the dye molecules is charge separation and electron injection from the dyes' lowest unoccupied molecular orbital (LUMO) to the oxide semiconductor's conduction band. This is strengthened by an initial intramolecular charge transfer within the dye molecule in which the LUMO should be located close to the anchoring group. Electron injection typically occurs on the sub-ps timescale, but it competes kinetically with other decay mechanisms taking place on the same timescale, such as aggregation-induced quenching, internal conversion and isomerization.[32,34-43] In this regard, a detailed study of the excited state dynamics in dye sensitizers is of great importance towards optimizing the photoconversion efficiency and design strategies for novel compounds with improved photovoltaic performance.

Typically, the photophysics of dye sensitizers, including excited state dynamics, is investigated in solutions and/or nanocrystalline semiconductor nanoparticles, such as TiO_2 and ZnO.[44-53] It is noted however, that the charge-transfer photophysics is affected, among others, by the deprotonation of the carboxylic group of the dyes. This acid-base equilibrium exists in solution and should be also considered when adsorbing dye onto the metal-oxide substrate. Shifting the equilibrium towards either side depends on the concentration of the solute as well as on the acidity or bacidity of the solvent. According to the Ostwald's law for weak acids, the neutral COOH form is dominant at high concentrations, while the equilibrium is shifted towards the anionic COO^- form at lower concentrations. Therefore, a thorough understanding of the photophysics of organic sensitizers may be more complicated than initially thought, but also it is of high importance since the equilibrium between neutral and anionic species influences the solar cell performance as well.[54-57] Ozawa et al. reported that the efficiency of the DSSCs based on the black dye (N749) becomes higher for solvents with a dielectric constant of about 20.[54] Tian et al. have shown that dichloromethane, used as a solvent of the dye bath for an organic dipolar sensitizer, shifts the equilibrium towards the neutral form and increases the solar cell efficiency compared to DSSCs obtained from tetrahydrofuran, acetonitrile or ethanol dye-baths.[55]

In a previous work of ours, the photophysics of three organic sensitizers bearing triphenylamine electron-donating group and benzothiazole acceptor has been studied by means of a variety of time resolved spectroscopies.[34] It was reported that these dyes exhibit ultrafast electron injection towards TiO_2, but the electron injection is operative also towards Al_2O_3, which is often used as a reference electrode. Here, we extend our previous work by investigating the photophysics of one of the benzothiazole-derived sensitizers (**BTZA-II**) in solutions of varying acidity and also by studying its solar cell performance resulting in a simple yet efficient way for improving the efficiency. The photophysics has been studied by stationary and time resolved spectroscopies in solutions of different concentrations as well as in mixtures of given solvents with acetic acid (AcOH) and the strong base, DBU (1,8-diazabicyclo-[5.4.0]undec-7-ene) in order to shed more light on the origin of fluorescence and the equilibrium between the neutral and anionic form. AcOH is added to the solutions in order to recover the neutral dye molecules (COOH form), while DBU was added to deprotonate a cyanoacrylic carboxylic group. For comparison, we also studied the photophysics of an organic sensitizer **Btz-NPh2** resembling the D-π-A framework of **BTZA-II**, but without the cyanoacrylic acid group. Finally, the effect of adding small amounts of AcOH to the initial dye bath on the solar cell performance was also investigated, showing a exceptional 58 % increase of the photoelectric conversion efficiency (η reaching a value of 4.9 %).

EXPERIMENTAL

Dye sensitizer and materials used for the fabrication of the DSSCs

The chemical structure and abbreviation of the organic sensitizers studied in this work are shown in Chart 1. **BTZA-II** was chosen for this study because a) it has similar structure with other well studied organic sensitizers bearing the triphenylamine electron donor[40,45,55] and b) its lifetime is in the range of 100 ps - 1 ns in both of the solvents used herein, i.e. toluene and acetonitrile, and therefore it is detectable with the Time Correlated Single Photon Counting (TCSPC) method. **BTZA-II** was synthesized according to the procedure described in our previous work,[34] while **Btz-NPh2** was prepared similarly by a Knoevenagel-type condensation between commercially available 2-metylbenzothiazole and 4-(N,N-diphenylamino)benzaldehyde.

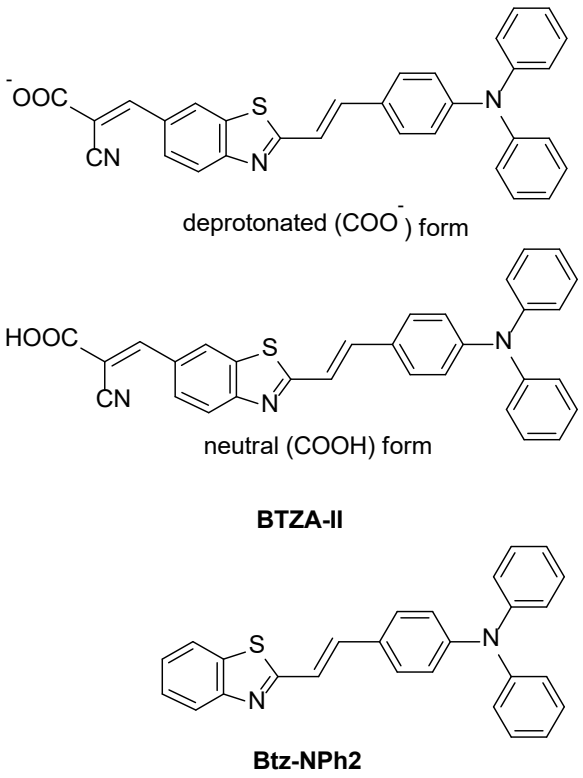

Chart 1. Structures of the benzothiazole-derived sensitizers studied in this work

Synthesis of 2-{2-[4-(*N*,*N*-diphenylamino)phenyl]vinyl}benzothiazole (**Btz-NPh2**): To a solution of 2-methylbenzothiazole (0.50 g, 3.35 mmol) in MeOH (6 mL) was added 4-(N,N-diphenylamino)benzaldehyde (0.92 g, 3.35 mmol) and solid NaOH (0.2 g, 5 mmol) as a base catalyst. The reaction mixture was stirred and heated to reflux. After refluxing for 12 h, 2 mL of MeOH was evaporated and the resulting solid was collected by filtration, washed and dried. The crude product was purified by column chromatography on silica gel (eluent: hexanes/etyl acetate = 4:1) to give **Btz-NPh2** (1.28 g, 95%) as a yellow solid; mp 154–156°C. ^{1}H NMR (300 MHz, $CDCl_3$, in ppm vs. TMS): δ = 7.96 (dd, 1H, J = 8.1 Hz, 0.6 Hz, H-7), 7.84 (dd, 1H, J = 8.1, 0.6 Hz, H-4), 7.48-7.42 (m, 1H, H-5), 7.43 (d, 2H, J = 8.7 Hz, H-2',H-6'), 7.37-7.31 (m, 1H, H-6), 7.29 (d, 1H, J = 15.3 Hz, H-ß), 7.32-7.24 (m, 4H, H-Ar), 7.14 (d, 2H, J = 8.7 Hz, H-3', H-5'), 7.15-7.03 (m, 6H, H-Ar), 7.06 (d, 1H, J = 15.3 Hz, H-α). ^{13}C NMR (75 MHz, $CDCl_3$, in ppm vs. TMS): δ = 167.51, 153.91, 149.08, 147.04, 137.31, 134 20, 129.35, 128.65, 128.41, 126.23, 125.07, 124.95, 123.76, 122.67, 122.23, 121.42, 119.77.

O,O'-Bis(2-aminopropyl) polypropylene glycol-block-polyethylene glycol-block-polypropylene glycol (Jeffamine® ED-600, M_r~600) and 3-isocyanatopropyltriethoxysilane (ICS; molar ratio ICS/diamine=2) were used for the synthesis of hybrid organic/inorganic material ED600-ICS necessary for quasi-solid state electrolyte. Commercial titanium(IV)

butoxide (Ti(OtBu)4, 97%, Aldrich), Pluronic P123 (5.800 g/mol, Aldrich), glacial acetic acid (AcOH, 99–100%, Aldrich) were used to prepare TiO_2 precursor sols. Finally, all solvents were purchased from Sigma-Aldrich and used as received. SnO_2:F transparent conductive electrodes (FTO, TECTM A8) 8 Ohm/square were purchased from Pilkington NSG Group.

Stationary spectroscopy

The UV-Vis absorption spectra were recorded by a Jasco V-650 UV-Vis spectrophotometer. The photoluminescence spectra were detected by a Fluoromax-4 spectrometer (Horiba).

Time resolved spectroscopy

The time resolved fluorescence measurements were performed with a TCSPC Fluorescence Lifetime Spectrometer (FluoTime 200, Picoquant) equipped with a Hamamatsu R3809U-5X series microchannel-plate photomultiplier.[58] The samples were excited by a LDH Series picosecond pulsed diode laser, with -excitation wavelength at 470 nm and energy per pulse of 0.05 – 0.15 nJ (Picoquant). The Instrument's Response Function (IRF) of the system was ~ 80 ps. Fluorescence dynamics were detected under magic angle conditions and the best fitting was determined by inspection of the residuals and through the χ^2 factor which should be smaller than 1.1. In all cases, single or bi-exponential dynamics were found to accurately reproduce the experimental decays. TCSPC method is a valuable tool for this study because it is highly sensitive and suitable for studying very dilute solutions.

Fabrication of the quasi-solid state dye-sensitized solar cells

Initially, the conductive glasses were cleaned with alkaline detergent, deionized water and acetone. For the preparation of the TiO_2 solution through the sol-gel technique, 0.49 g P-123 were diluted in 4 mL of n-propanol, followed by the addition of 0.4 mL glacial acetic acid and 0.37 mL of titanium(IV) butoxide under continuous stirring. For the formation of the working electrodes, this solution was spin coated on the FTO glasses at 1200 rpm for 10 s and consequently the films were annealed at 500^{o}C for 10 min. These two steps were repeated several times until ~3 micrometer TiO_2 films were obtained. The dye sensitizer was diluted in toluene to a concentration of 0.5 mM. For the sensitization process, the photoanodes were immersed in the dye solution (5 mL) for 30 minutes and then they were rinsed with the same solvent and dried to remove any solvent residues from the pores of the films. The platinum counter electrodes were formed through thermal decomposition of H_2PtCl_6 solution (5 mg

H_2PtCl_6/1 ml of n-propanol). Briefly, a few drops of the platinum solution were casted on top of the conductive glasses which were then annealed at 500ºC for 10 min.

The procedure for the synthesis of the hybrid organic-inorganic material used for the jellification process of the electrolyte and the completed electrolyte solution are described elsewhere.[59] For the fabrication of the quasi-solid state dye-sensitized solar cells, a couple of drops of the electrolyte solution are placed onto the sensitized working electrode and the platinized counter electrode is placed by hand over the photoanode in a sandwich structure. The two electrodes are stuck together through -Si-O-Si- bonds developed by the presence of the hybrid organic-inorganic material of the electrolyte solution.

Characterization methods for the quasi-solid state DSSCs

For the electrical characterization, the DSSCs were illuminated with Xe light using a Solar Light Co. solar simulator (model 16S-300). Light intensity was kept constant at 100 $mWcm^{-2}$ measured with Newport power meter (Model 843-R). The current density-voltage (*J-V*) characteristic curves were recorded by connecting the devices to a Keithley Source Meter (model 2601A) controlled by Keithley computer software (LabTracer). The DSSCs' active area was restricted to 0.18 cm^2 by using an appropriate mask. In order to avoid any misleading results, each DSSC device was prepared in triplicate and tested under the same conditions. The electrical parameters determined by the *J-V* plots were the short-circuit current density (J_{SC}), the open circuit voltage (V_{OC}), the fill factor (FF) and the overall cell conversion efficiency (η%). Electrochemical impedance spectroscopy measurements (EIS) were performed by using Metrohm Autolab 3.v potentiostat galvanostat (Model PGSTAT 128N) under light conditions. The cells were illuminated using the same Xe light source that was used for the *J-V* curves, without the use of a mask. The frequency range which was applied was 100 kHz-0.01 Hz using a perturbation of ±10 mV over the open circuit potential. The obtained experimental data were fitted using Nova 1.10 software.

Computational details

The structure of **BTZA-II** was optimized by using density functional theory (DFT) at the B3LYP/TZVP level in the Gaussian 09.[60] Vertical excitation energies and adiabatic dipole moment change ($\Delta\mu_{01}$) between the ground state and the first excited state were computed at the time-dependent DFT level, employing the modified CAM-B3LYP functional[61] with the following parameters: $\alpha = 0.19$, $\beta = 0.33$, $\gamma = 0.33$, and the TZVP basis set for all atoms. Bulk solvent effects were simulated using the integral equation formalism of the polarizable

continuum model (IEF-PCM).[62] A number of conformational isomers were examined, and the computed excitation energies were Boltzmann-averaged (at 298 K). The Onsager cavity radius a_0 was evaluated by a gas-phase calculation of molecular volume. This was realized employing Monte-Carlo integration, as implemented in the Gaussian 09 program package, by specifying the keyword *volume=tight*.

RESULTS AND DISCUSSION

Stationary absorption and fluorescence spectra

The absorption and fluorescence spectra of **BTZA-II** were studied in apolar toluene (ε_r=2.38) and highly polar acetonitrile (ε_r=37.5). Apart from the bulk solvent polarity, the acidity of the two solvents should be also considered, as this affects the COO^-/COOH dye equilibrium and thus also the photophysical properties. The Kamlet-Taft parameters for toluene (α=0 and β=0.11) points to its very weak H-acceptor ability, while acetonitrile (α=0.19 and β=0.4) is considered as much stronger base (H-acceptor) and a very weak H-donor.[63]

Initially, the solute concentration was varied by two orders of magnitude (5×10^{-7} M to 5×10^{-5} M) to determine the effect of the acid-base COOH/COO^- equilibrium on the spectra. In toluene, the absorption spectra exhibit a peak at 440 nm for the lowest concentration (5×10^{-7} M) and show a red-shift of 9 nm upon increasing the concentration (Figure 1a). In Table 1, the photophysical parameters for the concentration of 5×10^{-6} M are summarized. As reported previously, the anionic (deprotonated) form absorbs at shorter wavelengths than the neutral one.[34] Therefore, the spectrum at the lowest concentration is dominated by the absorption of the anionic form, while the red-shift is due to the increased portion of neutral dye molecules.

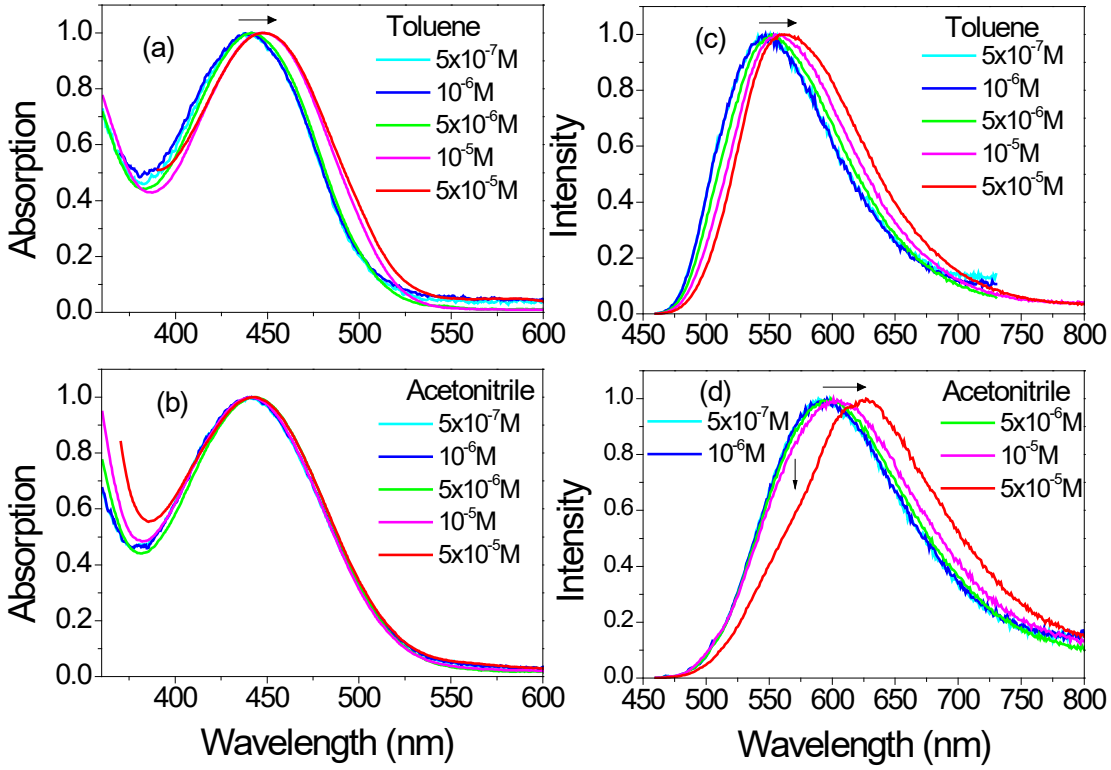

Figure 1. Absorption (a) , (b) and fluorescence (c) , (d) spectra of **BTZA-II** in toluene and acetonitrile solutions with different concentrations. The arrows indicate the changes of the spectra upon increasing the concentration.

Table 1. Photophysical parameters of **BTZA-II** solutions with a dye concentration of 5×10^{-6}M.[a]

Sample	λ_{abs} (nm)	λ_{fluor} (nm)
BTZA-II/Toluene	441	552
BTZA-II/Toluene + 5 μL DBU	428	517
BTZA-II/Toluene + 5 μL AcOH	468	586
BTZA-II/Acetonitrile	442	598
BTZA-II/Acetonitrile + 5 μL DBU	421	598
BTZA-II/Acetonitrile + 5 μL AcOH	445	610

[a] The volume of the initial toluene solutions was 3 ml.

The fluorescence spectra in toluene show a very similar behavior. Specifically, the fluorescence exhibits a peak at 551 nm for $c=5\times10^{-7}$M, while a 10 nm red-shift (without any change in the width of the spectra) is observed upon increasing the dye concentration to 5×10^{-5}M (Figure 1c). A different behavior is observed in acetonitrile. The absorption spectrum shows a

peak at 442 nm and does not change upon increasing the concentration (Figure 1b). This coincides with the much stronger H-acceptor ability of acetonitrile as compared to toluene that shifts the equilibrium towards the anionic form even at higher concentrations. Moreover, the fluorescence spectra, exhibit a red-shift, especially for the highest concentration used, but in contrast to toluene, this is accompanied by a change in the spectral profile (Figure 1d). This change is mostly attributed to a decrease of the fluorescence intensity at shorter wavelengths (where the anionic form emits), leading to a narrowed spectrum. These findings indicate that although the anionic population in acetonitrile is not changed upon increasing the concentration, the fluorescence becomes less intense. This quenching is in agreement with the time resolved fluorescence results (*vide infra*).

The aforementioned different behavior observed in the two solvents was further investigated by means of the excitation spectra ($c=5\times10^{-6}$M) (Figure 2). In toluene, the low-energy peaks of the excitation and absorption spectra coincide. The absorption is due to both neutral molecules and anions of the dye. According to the excitation spectrum, both these species contribute to the emission. However, the contribution from the low-energy neutral form is higher as revealed by the slight red-shift of the excitation spectrum. On the other hand, the excitation spectrum in acetonitrile is significantly shifted towards shorter wavelengths (by ~20 nm) as compared to the absorption spectrum, and it is also narrower. This clearly indicates that although both species absorb, the fluorescence stems from the higher energy one, which corresponds to the anion, while the neutral form in acetonitrile is non- or weakly fluorescent. This explains the observed behavior of the fluorescence spectrum upon increasing the concentration. At higher concentrations, the amount of anionic form is reduced and the intensity of the high energy part of the spectrum decreases leading to the apparent red-shift (Figure 1d). This is further investigated by adding DBU base to the solutions.

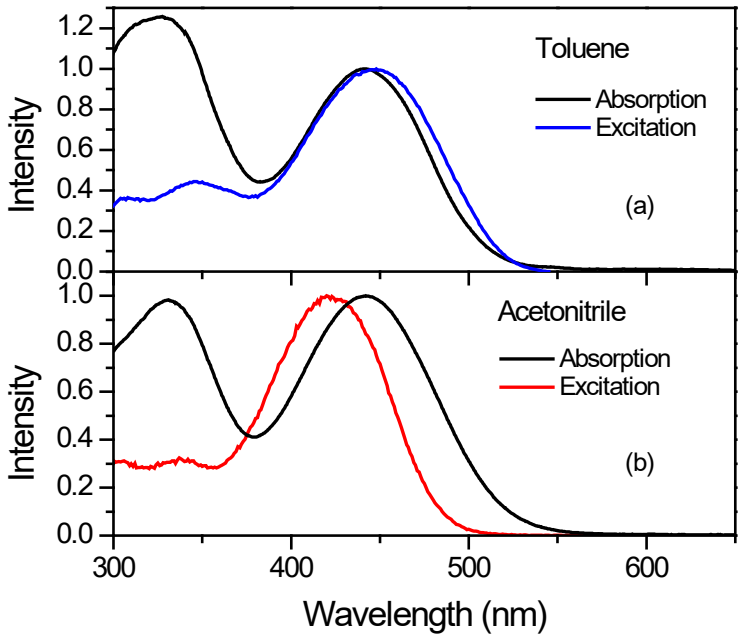

Figure 2. Fluorescence excitation spectra of **BTZA-II** solutions with concentration 5×10^{-6}M in (a) toluene and (b) acetonitrile. The absorption spectra are shown for comparison.

In order to increase the portion of anions in the solutions, without the need of decreasing the concentration, a small amount of DBU was added. The addition of DBU leads to a hypsochromic shift of the absorption spectrum due to the shift of the equilibrium towards the anionic (deprotonated) form. The spectra for 5×10^{-6}M solutions with and without DBU are shown in Figures 3a and 3b. The changes in the absorption spectra upon addition of DBU are qualitatively similar in both solvents (Table 1). A similar hypsochromic shift takes place even for the more concentrated initial solutions (5×10^{-5}M) in toluene (Figure S1), where the equilibrium is initially shifted towards the neutral form. However, the excitation and fluorescence spectra after addition of DBU display a different behavior in toluene and acetonitrile, revealing the different nature of the existing species in each solvent. In toluene, both excitation and fluorescence spectra exhibit a hypsochromic-shift upon addition of DBU, indicative of the generation of anions, which dominate the emission process (Figures 3c and 3e). In acetonitrile, the excitation and fluorescence spectra do not change upon addition of DBU (Figures 3d and 3f). This indicates that even in the initial acetonitrile solution without DBU, the dominant contribution to the fluorescence originates from the anionic form, while the neutral (COOH) species has a very small fluorescence quantum yield. Therefore, the addition of DBU does not cause any change in the spectra.

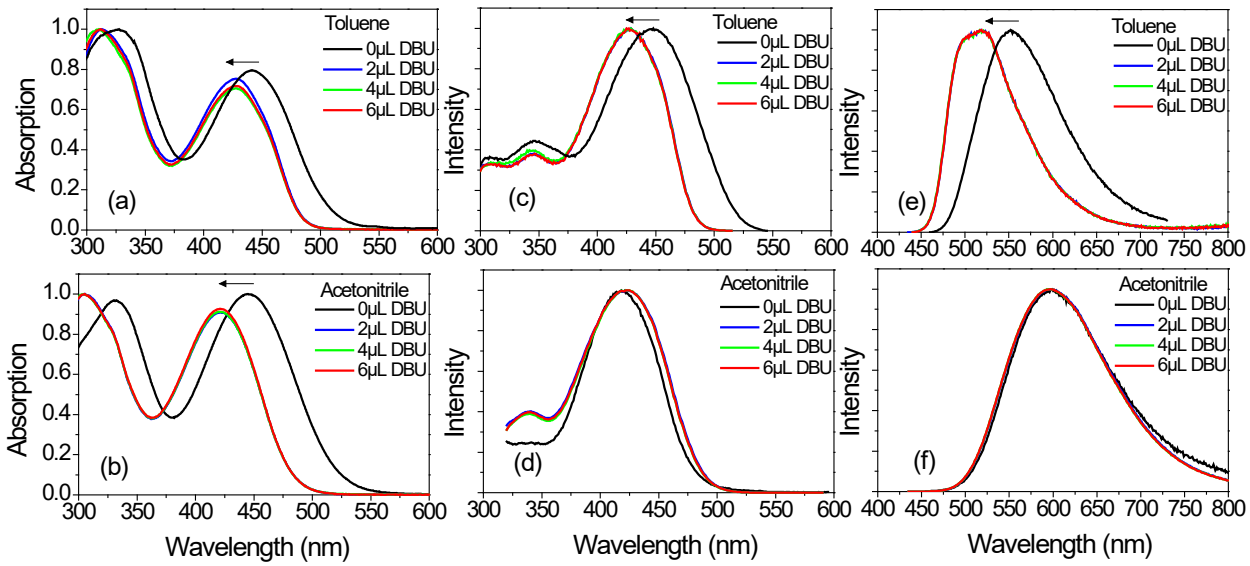

Figure 3. Absorption (a), (b), fluorescence excitation (c), (d) and fluorescence (e), (f) spectra of **BTZA-II** in toluene and acetonitrile with concentration 5×10^{-6}M without and with various amounts of DBU (the volume of a dye-solution was 3 mL) . The arrows show the change of the spectra upon adding DBU.

Figures S2a and S2b show the dependence of the excitation spectra on the detection wavelength in toluene solutions without and with DBU. In the former case, the excitation spectra display a red-shift upon increasing the detection wavelength indicative of an inhomogeneous broadening and the existence of different species responsible for the emission, which are the neutral and anionic form (Figure S2a). However, when DBU is added, the excitation spectra do not display such a shift (Figure S2b). This is ascribed to the existence of a single emitting species in the DBU solutions, corresponding to the anionic form.

For a further investigation of the effect of the portions of COOH and COO^- dye forms on the photophysical properties, the absorption and emission spectra of **BTZA-II** with and without DBU were detected also in various organic solvents with different polarity. The results of this study are presented in Table S1 and Figure S3. Hence, plotting Stokes shifts $\boldsymbol{\nu_A - \nu_F}$ vs. the solvent orientation polarizability Δf allowed us to determine the difference between the dipole moment of the excited and ground state $\Delta\mu = \mu_E - \mu_G$ through the Lippert-Mataga equation[64-66]:

$$\nu_A - \nu_F = \frac{2(\mu_E - \mu_G)^2}{hca_0^3}\Delta f + constant \qquad (1)$$

Note that while this plot for **BTZA-II** in the presence of DBU (dissociated form of the sensitizer) clearly shows a linear dependence of the Stokes shifts on the solvent polarizability

with a slope of 8644 cm^{-1} (R^2=0.830), data points in the Lippert-Mataga plot (LMP) for **BTZA-II** without DBU are considerably spread around the regression line (R^2=0.505). The latter can be understood as there is a different ratio between dissociated and non-dissociated form of the dye (anion and neutral), depending on the nature of solvent. Using a cavity radius, a_0, of 6.29 Å for the anion of **BTZA-II** (estimated from the molecular volume calculated by Monte-Carlo integration of the electronic density) the LMP gives the dipole moment change, $\Delta\mu$, of 15.6 D. This is in reasonable agreement with the value of 13.2 D obtained by our quantum-chemical calculations at the mCAM-B3LYP/TZVP level using a PCM solvation model.

In order to investigate the photophysical properties of **BTZA-II** in its neutral "non-deprotonated" form, small amounts of AcOH were added to toluene and acetonitrile solutions. The absorption spectrum in toluene exhibits a red-shift even for the smallest amount of acetic acid (1 µL) meaning that the equilibrium shifts towards the neutral form (Figure 4a). The same conclusions are also drawn by inspecting the excitation and fluorescence spectra in toluene and toluene+AcOH where a red-shift is also exhibited (Figures 4 c, e).

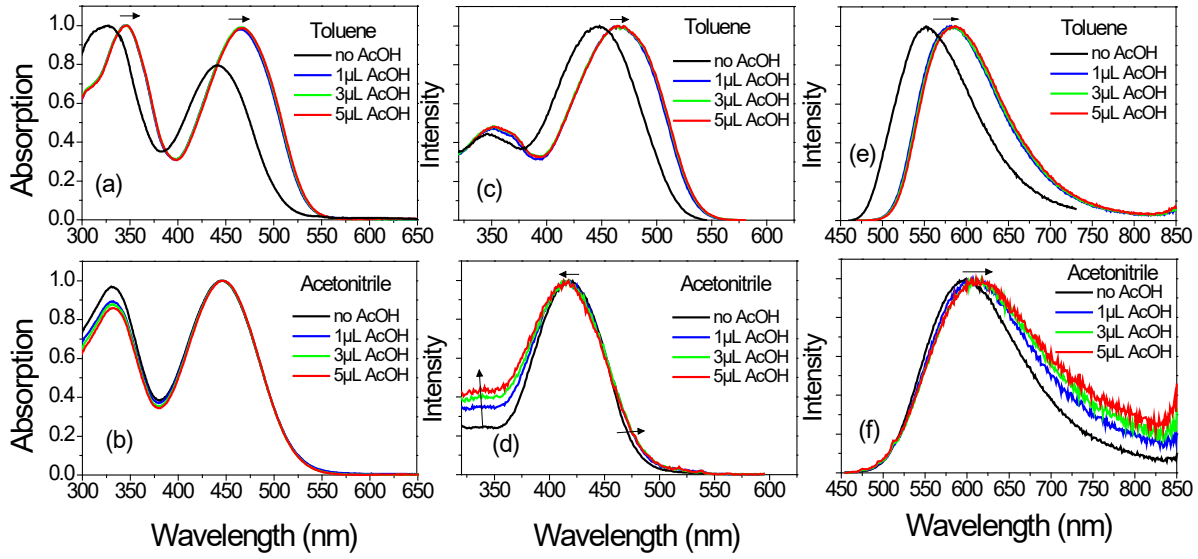

Figure 4. Absorption (a), (b), excitation (c), (d) and fluorescence spectra (e), (f) of **BTZA-II** in toluene and acetonitrile before and after addition of various amounts of AcOH (the volume of a dye-solution was 3 mL). The small arrows indicate the change of the spectra upon increasing the volume of acetic acid in the solutions.

On the other hand, in acetonitrile, no significant spectral shifts in absorption, excitation and fluorescence spectra are observed as shown in Figures 4 b, d and f. However, we note a significant drop in the fluorescence intensity upon adding AcOH, which is not obvious in the normalized spectra (see Figure S4). This is primarily ascribed to the generation of weakly

fluorescent neutral species at the expense of the fluorescent anions. This is in agreement with the excited state dynamics which exhibit a significant decrease of the lifetime when AcOH is added (*vide infra*). Similar behavior was reported for the well-known dye sensitizer D149 and indicates that the dye's fluorescence is quenched by acid via proton transfer.[46]

The excitation spectra of **BTZA-II** in toluene solutions with AcOH provide another indication that a single species exist in this solvent. Particularly, the spectra upon adding AcOH exhibit only a very small shift with varying the detection wavelength. This means that the equilibrium is shifted almost quantitatively towards the neutral form (Figure S2c).

In order to unambiguously determine that the spectral changes are solely related to the COO^-/COOH equilibrium and the benzothiazole nitrogen as a potential Brønsted-base center is not responsible for the observations mentioned above, similar experiments were performed also for the **Btz-NPh2** analogue. The results are presented in Figure S5. Hence, it is clear that spectral changes upon addition of AcOH are minimal (< 1 nm), meaning that the protonation of the nitrogen atom of the benzothiazole scaffold upon treatment with AcOH is negligible. This coincides with the weak acidic nature of acetic acid (pK_a = 4.76), which is not strong enough to protonate the azole nitrogen in the quantities used. Keeping with expectations, no spectral changes were observed upon addition of DBU, since **Btz-NPh2** contains no protic group.

Fluorescence dynamics

According to the results of stationary spectroscopy, the fluorescence spectra upon increasing the concentration exhibit a red-shift in both solvents, while in acetonitrile, a decrease of the intensity was also observed. The ns fluorescence dynamics of **BTZA-II** solutions with different concentrations are shown in Figure 5. These were analyzed by a global fitting procedure by means of a bi-exponential function in order to determine the lifetime of the anionic and neutral forms and to examine the dependence of their pre-exponential factors on the concentration (Table 2). The dynamics in toluene become slower upon increasing the concentration, while in acetonitrile they are accelerated. This is a clear indication of the different photophysics of the anion and neutral form in these solvents. In toluene, two components are observed with time constants of 1.1 and 1.9 ns. The pre-exponential factor of the 1.1 ns component decreases with concentration and is attributed to the anion lifetime in toluene, while the 1.9 ns component, whose amplitude increases, is attributed to the lifetime of the neutral form. On the other hand, in acetonitrile the two components have lifetimes of 0.5 and 2.0 ns, respectively. The longer component is very close to that found in toluene, however its amplitude decreases with

concentration and is considered as the lifetime of the anion. The neutral form has a lifetime of 0.5 ns and its fluorescence is greatly quenched in acetonitrile.

Another way for determining the contribution of the anionic and neutral form is by detecting the dynamics at various emission wavelengths. It is expected that the anionic and neutral forms contribute to the fluorescence at short and long wavelengths, respectively. Indeed, as observed in Figure 6, the dynamics for a concentration of 5×10^{-6} M, become slower/faster at longer wavelengths in toluene/acetonitrile due to the increased contribution of the neutral form.

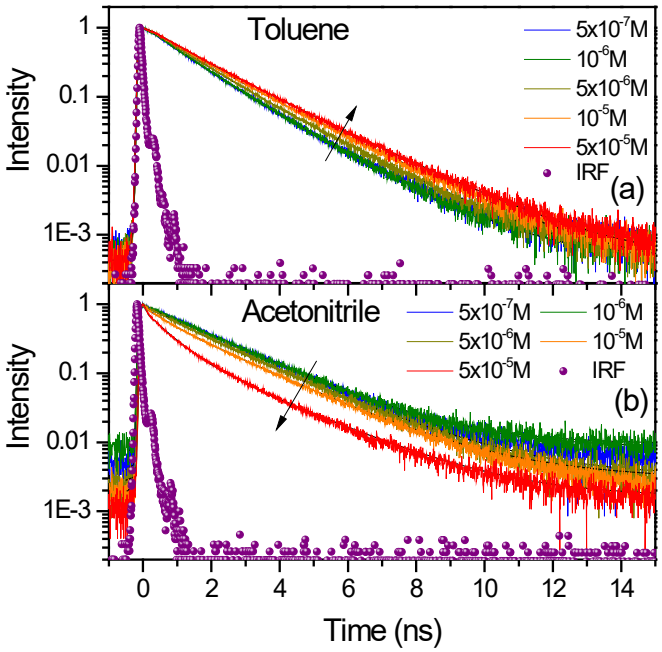

Figure 5. Fluorescence dynamics of **BTZA-II** in (a) toluene and (b) acetonitrile for different concentrations upon detection at the peak of the fluorescence spectra. The arrows show the change of the fluorescence dynamics upon increasing the concentration.

Table 2. Fitting parameters of the dynamics of **BTZA-II** in toluene and acetonitrile for different concentrations obtained after a global analysis.

Sample		λ_{det} (nm)	A_1	τ_1 (ns)	A_2	τ_2 (ns)
BTZA-II/ Toluene	5×10^{-7}M	550	0.75	1.1	0.25	1.9
	1×10^{-6}M	550	0.75		0.25	
	5×10^{-6}M	550	0.64		0.36	
	1×10^{-5}M	555	0.48		0.52	
	5×10^{-5}M	565	0.37		0.63	
BTZA-II/ Acetonitrile	5×10^{-7}M	600	0.09	0.5	0.91	2.0
	1×10^{-6}M	600	0.09		0.91	
	5×10^{-6}M	600	0.21		0.79	
	1×10^{-5}M	605	0.34		0.66	
	5×10^{-5}M	630	0.68		0.32	

For the dynamics in toluene, a global fitting procedure was performed to analyse the data and the fitting parameters are summarized in Table S2. This analysis revealed two decay mechanisms with 1.1 and 1.8 ns lifetimes, which are very similar to those found for the solutions of different concentrations. The amplitude of the 1.8 ns component increases at longer wavelengths confirming that this is the lifetime of the neutral form in toluene, while the contribution of the 1.1 ns component is significant at short wavelengths and is ascribed to the emission of the anion.

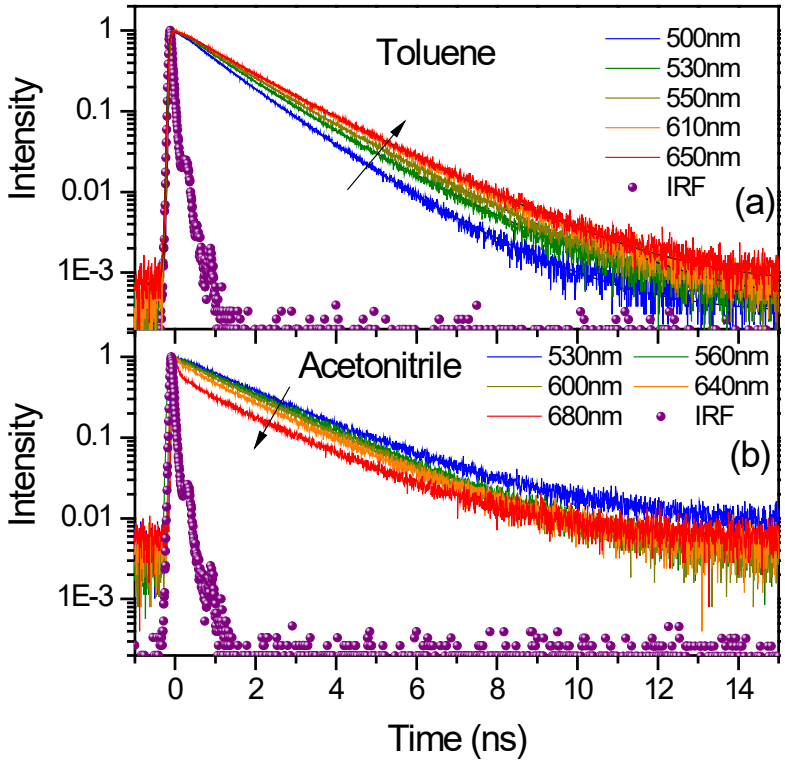

Figure 6. Fluorescence dynamics of **BTZA-II** in (a) toluene and (b) acetonitrile (5×10^{-6}M) at different detection wavelengths. The arrows indicate the change of the decays by increasing the emission wavelength.

As shown in the SI (Table S3), the same behavior is observed for all the other concentrations in toluene (i.e. two components of ~ 1 and ~ 1.8 ns are found where the contribution of the former decrease and that of the latter increase at longer wavelengths). The dynamics in acetonitrile, could not be properly fitted by a global analysis, because of the greatly different dynamics at short and long wavelengths. However, it is clear that at longer wavelengths the dynamics are accelerated.

Before studying the excited state dynamics of **BTZA-II** upon adding DBU and AcOH, the effect of these additives on the photodynamics has been examined for the reference compound **Btz-NPh2**. As shown in Figure S6, the dynamics of **Btz-NPh2** in toluene (5×10^{-6}M) are not

affected by addition of acid/base, proving that the protonation of the N atom of benzothiazole is negligible. Similar results were also observed for acetonitrile solution.

Similar conclusions as those obtained by stationary spectroscopy emerge for **BTZA-II** by investigating the TCSPC measurements upon addition of DBU, as can be seen in Figure 7 for a concentration of 5×10^{-6}M (the fitting parameters are collected in Table S4). In toluene, the decays become faster when DBU is added, indicating that the emission stems from the anions having a shorter lifetime than the neutral "non-deprotonated" form. In more details, a global analysis of the dynamics in toluene+DBU solutions, revealed that the long component of ~ 1.8 ns due to the neutral form is completely absent. Besides, the dynamics of the anionic form in toluene+DBU could not be fitted with a single-exponential function. Thus, a bi-exponential one was used, revealing 0.9 and 0.5 ns components. The former is close to the 1.1 ns lifetime of the anion in neat toluene solution although slightly smaller. The nature of the latter and faster component (0.5 ns) needs further investigation. On the other hand, the lifetimes in acetonitrile and acetonitrile+DBU are virtually identical, as shown in Figure 7b (the ~ 2 ns component is attributed to the lifetime of the anionic form in acetonitrile, Table 2). This is consistent with the findings from stationary spectra, which also showed negligible changes upon adding DBU, confirming the dominance of anionic species in acetonitrile solutions.

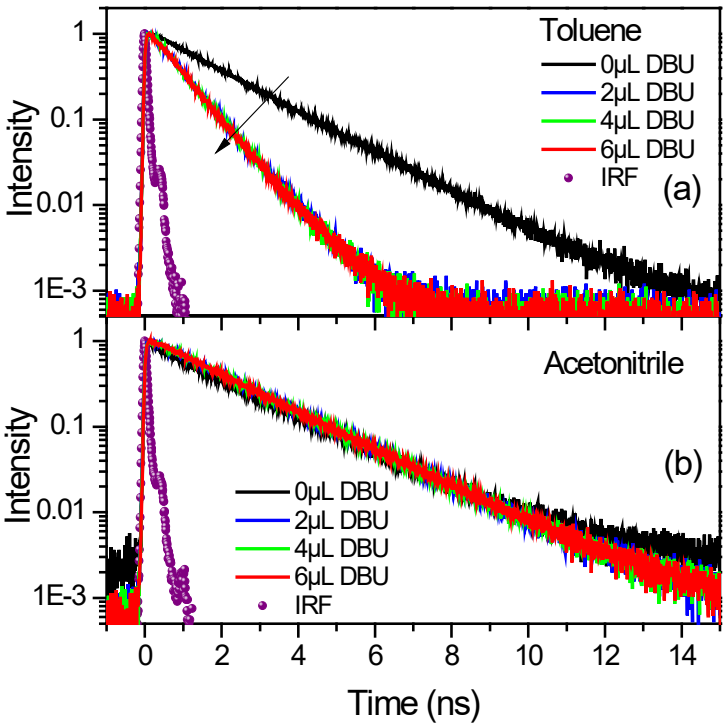

Figure 7. Fluorescence decays of **BTZA-II** in 5×10^{-6}M (a) toluene and (b) acetonitrile solutions before and after addition of various amounts of DBU. The arrow in (a) indicates the change of the dynamics upon adding DBU.

In order to test the influence of a base additive in concentrated acetonitrile solutions, 6 μL of DBU were added to a 5×10^{-5}M solution of **BTZA-II**. At this high concentration, the fluorescence of **BTZA-II** in neat acetonitrile solution is quenched because of the effect of protons as discussed previously (Figure 5b), showing that the neutral form in acetonitrile is weakly fluorescent. Upon addition of DBU, the **BTZA-II** molecules are deprotonated quantitatively even at this high concentration and the fluorescence intensity as well as the lifetime increase (Figure S7).

Further, the dependence of the dynamics in toluene and acetonitrile solutions with DBU on emission wavelength was investigated so that the contribution of neutral species was determined. The results are shown in Figure 8, indicating clearly that the dynamics and lifetime are independent on the wavelength used (i.e. the contribution of neutral "non-deprotonated" species is completely absent even at longer wavelengths).

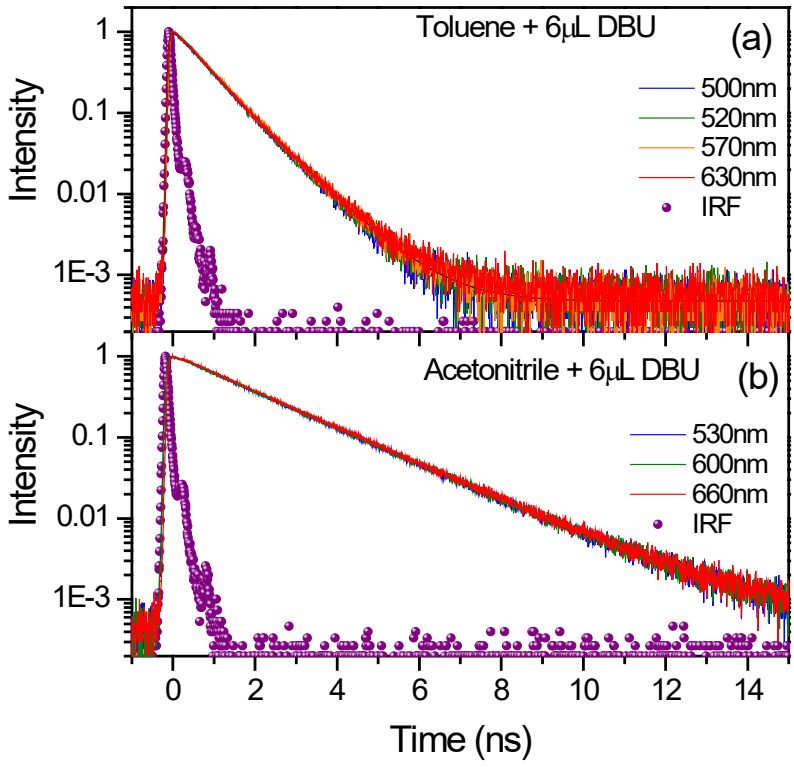

Figure 8. Fluorescence decays of **BTZA-II** in 5×10^{-6}M (a) toluene and (b) acetonitrile solutions with 6 μL of DBU at different detection wavelengths.

As mentioned above, the addition of a small amount of AcOH recovers the protonated COOH form of **BTZA-II** molecules. The steady state results in toluene upon addition of acid showed that protonation leads to a red-shift of the spectra (Figure 4e). A similar behavior was exhibited by increasing the concentration (Figure 1c). The dynamics upon protonation due to

increased concentration showed a decrease of the contribution of the anionic form (Figure 5a and Table 2). This behavior is more pronounced upon adding very small amounts of acid. Specifically, as shown in Figure 9a and Table S5, the contribution of the anion with 1.1 ns is totally absent when acid is added and the fluorescence decay is single exponential due to emission by the neutral species with lifetime of ~ 1.9 ns.

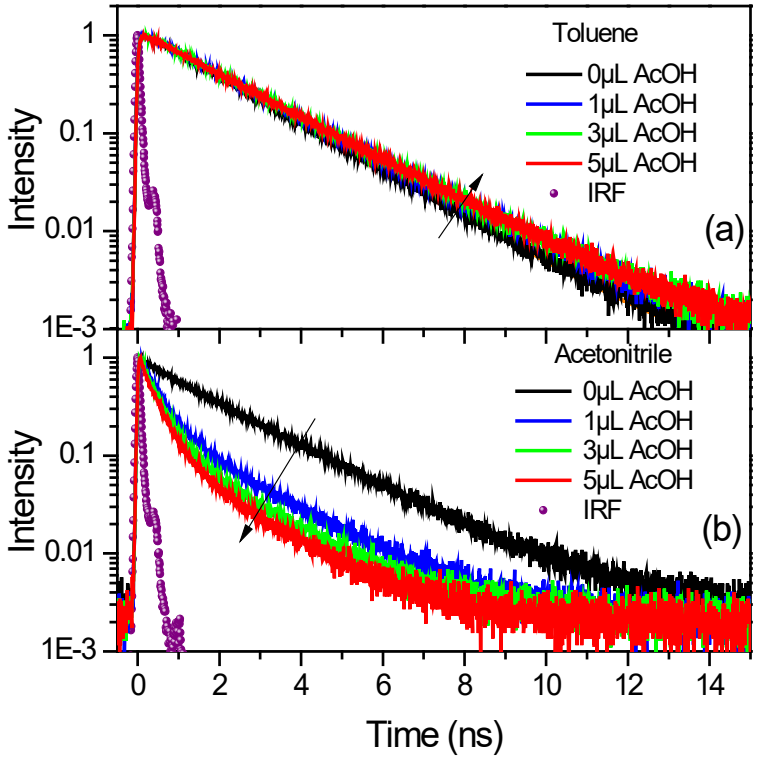

Figure 9. Fluorescence decays of **BTZA-II** detected at the peaks of the fluorescence spectra in 5×10^{-6}M (a) toluene and (b) acetonitrile solutions before and after addition of various amounts of AcOH. The arrows show the change of dynamics upon increasing the amount of acid.

As expected, the behavior in acetonitrile is different. Similarly to the decrease of the fluorescence intensity upon addition of AcOH to acetonitrile solutions, as discussed before (Figure S4), the excited state dynamics become highly bi-exponential and exhibit a significant decrease of the lifetime when AcOH is added (Figure 9b, Table S5). This behavior resembles the one in concentrated solutions meaning that the fluorescence is quenched by protons. The global fitting analysis revealed again two components with lifetimes 0.4 and 2.0 ns due to the neutral and anion species. The contribution of the weakly fluorescent neutral form in acetonitrile increased with acid leading to the overall decrease of intensity.

Solar cell performance

In respect to the abovementioned findings, we decided to examine the effect of adding small amounts of AcOH to the dye solutions on the performance of solar cell devices. Although the solar cell efficiency was studied in the past by using different solvents in the initial dye bath,[54-57] the effect of external acid added to the dye bath has not been investigated so far to the best of our knowledge. On the other hand, the influence of AcOH on the properties of the TiO_2 electrodes has been addressed.[67,68] Here, DSSCs were prepared from initial solutions of **BTZA-II** in toluene with and without the presence of AcOH. The AcOH was added in amounts 10 μL, 50 μL and 100 μL to 5 mL of **BTZA-II** solutions in toluene (with c = 0.5 mM), that corresponds to about 70, 350 and 700 equivalents of AcOH with respect the sensitizer molecules in a dye-bath. The results are presented in Figure 10a and Table 3. The photoconversion efficiency for cells prepared from neat toluene solution of **BTZA-II** was found 3.1 %, while a significant increase was observed for a mixture 5 mL toluene + 10μL of AcOH, where the efficiency reached a value of 4.9 %. This 58 % increase of the efficiency is of great importance taking into account the nontoxicity of the additive agent and simplicity of the process used. The significant photoelectric conversion enhancement can be attributed to increase of both J_{SC} and V_{oc}, the former being, however, more dominant. The small V_{oc} enhancement is most likely due to the decrease in electron-hole recombination from the conduction band of the TiO_2 film to I_3^- in the electrolyte. In other words, the increasing density of the dye adsorption onto the TiO_2 electrode may insulate the TiO_2 surface from the electrolyte, which in turn hinders the electron transfer from the TiO_2 surface to the I_3^- ions.[69] However, when the amount of AcOH is further increased, the efficiency drops. The explanation is in line with poor adsorption of the dye on the surface of TiO_2 when using a larger excess of AcOH. For an additional verification of the enhanced performance of the cells prepared from toluene +10 μL acid, *J-V* measurements have been carried out in dark. They clearly indicate that the electron leakage in the cell made from toluene in the presence of 10 μL acid is noticeably smaller (Figure S8). The absorption spectra of the sensitized films prepared from toluene+AcOH vs. toluene solutions showed an increase of the absorption efficiency pointing to a better adsorption of the neutral species, existing in toluene+AcOH solutions, on TiO_2 (Figure S9). The higher absorption of the sensitized films prepared from toluene+acid is in agreement with findings of Suresh et al.[70] They have reported that a TiO_2 adsorbed triphenylamine dye with neutral (COOH) anchoring group has higher absorbance than then anionic (COO^-) form, which was attributed on the basis of FTIR spectra to the nature of the carboxyl binding to the semiconductor surface. Specifically, the anionic form showed a bidentate binding with the surface of TiO_2, whereas the dye with a COOH anchoring group exhibited both

mono- and bidentate binding modes. In this way, despite the fact of a stronger binding of the anionic species with the TiO_2 surface, the "non-deprotonated" (COOH) dye form achieves an increased loading. In order to examine whether the addition of acid in the initial toluene solution, had an influence on the excited state dynamics of **BTZA-II**/TiO_2 films, we performed time resolved fluorescence measurements on the films (Figure S10). The dynamics were detected at 650 nm, which is the peak of the films' fluorescence spectra. Although, the differences are not extensive, the decay for **BTZA-II**/TiO_2 film prepared from toluene+AcOH was faster pointing to more efficient electron injection dynamics from the dye's LUMO to the conduction band of TiO_2. This conclusion becomes more unambiguous taking into account that the neutral form, whose concentration is increased with the addition of acid, has a longer fluorescence lifetime. The above results lead to the conclusion that addition of an appropriate amount of AcOH (corresponding to about 70 molar equiv of the dye used) to the initial bath, suppresses the deprotonation of the dye molecules and increases significantly the solar cell efficiency by both increasing the absorption and the electron injection efficiency.

Ito et al. have reported that AcOH can be adsorbed on the surface of TiO_2 and prohibits each TiO_2 particle from the aggregation.[68] In order to test whether the AcOH molecules play a similar role on dye molecules by prohibiting their aggregation, we prepared DSSCs from toluene solutions using the well-known co-adsorbent chenodeoxycholic acid (CDCA).

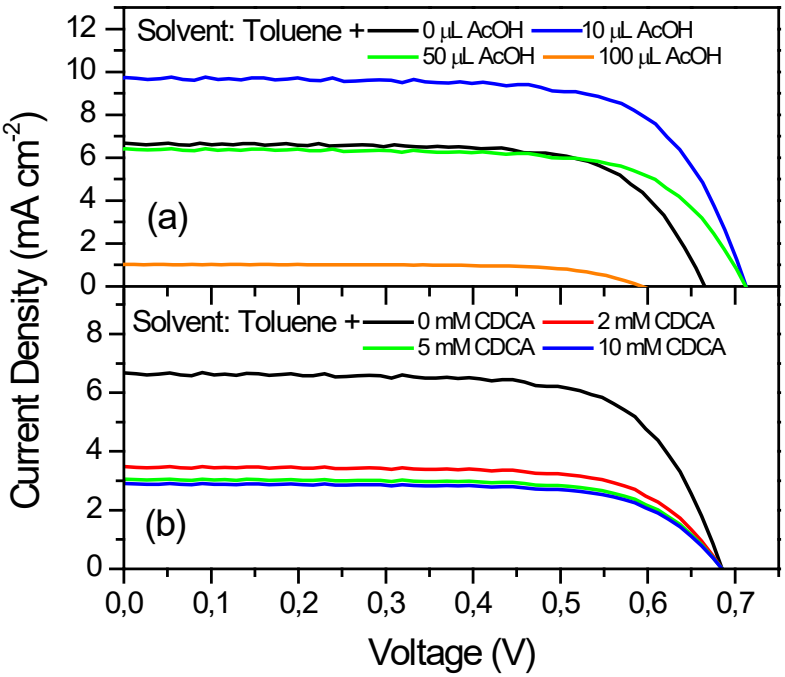

Figure 10. Current density vs. voltage curves of DSSCs with **BTZA-II** sensitizer prepared from toluene solutions with different amounts of (a) AcOH and (b) CDCA co-adsorbent.

Table 3. Solar cells parameters for DSSCs sensitized with **BTZA-II** from toluene solutions with various amounts of AcOH and CDCA co-adsorbent. [a]

Solvent	J_{SC} (mA/cm^2)	V_{oc} (Volts)	*FF*	η (%)
Toluene	6.70	0.66	0.70	3.1
Toluene+10 μL AcOH	9.75	0.71	0.71	4.9
Toluene+50 μL AcOH	6.41	0.71	0.71	3.2
Toluene+100 μL AcOH	1.02	0.58	0.70	0.42
Toluene+2 mM CDCA	3.47	0.67	0.70	1.6
Toluene+5 mM CDCA	3.05	0.66	0.70	1.4
Toluene+10 mM CDCA	2.90	0.67	0.70	1.4

[a] Variable amounts of AcOH and CDCA were added to 5 mL of the initial toluene solution of **BTZA-II** with *c*=0.5 mM. CDCA was added as a solid in such amount, that its concentration in the dye-bath reached a value of 2 mM, 5 mM or 10 mM.

CDCA was routinely used in the past to induce moderate to large increases in the solar cell efficiency by reducing dye aggregation on the surface of TiO_2.[71-77] Here, various amounts of CDCA were added to the dye bath before adsorption on the TiO_2 surface. The *J-V* curves are shown in Figure 10b. In all cases, the solar cell efficiency is significantly reduced compared to the solar cell prepared by using toluene solutions without CDCA. This is a consequence of the reduced light absorption by the **BTZA-II** films when CDCA is co-adsorbed on TiO_2 (Figure S11). Overall, it is evident that the significant increase of the solar cell efficiency upon adding AcOH to the dye solutions cannot be primarily attributed to the co-adsorption of the acid molecules and the suppression of dye aggregation since that would result in a decrease of absorption efficiency of the sensitized TiO_2 films as with CDCA. Instead, it is considered as a consequence of the protonation of the dye COO^- species in the toluene solution indicating that the neutral molecules are better adsorbed on the TiO_2 nanoparticles providing enhanced light absorption, faster electron injection and finally more than 50% increased solar cell efficiency. Preliminary results have shown that a similar increase of the solar cell efficiency, after addition of an optimal amount of AcOH, can be achieved by using different solvents in the initial dye solutions and this simple procedure works also for other dyes comprising a cyanoacrylic acid group leading to an increase of both J_{SC} and V_{oc} (Figure S12).

Table 4. EIS fitting parameters for DSSCs sensitized with **BTZA-II** from toluene solutions with various amounts of AcOH.

DSSC sample	R_h (Ω)	R_{pt} (Ω)	C_{pt} (10^{-5}F)	R_{tr} (Ω)	C_{tr} (10^{-3}F)	R_{dif} (Ω)	C_{dif} (10^{-3}F)
0 μL AcOH	11.9	1.96	3.10	8.53	3.80	2.05	3.10
10 μL AcOH	11.7	2.05	2.84	1.49	3.08	2.10	3.82
50 μL AcOH	11.6	2.81	2.34	7.89	3.34	2.97	3.20
100 μL AcOH	11.4	2.68	2.00	9.94	3.52	2.47	4.60

Electrochemical impedance spectroscopy (EIS) measurements were recorded under simulated solar light to explore the charge transfer process in DSSCs made with **BTZA-II** dye adsorbed on TiO_2 films using different quantities of AcOH in the original dye's solution. The impedance spectra of all DSSCs are plotted with Nyquist plots and are presented in Figure 11a. The left semicircle of Nyquist plot represents the charge-transfer resistance at the electrolyte/counter electrode interface (R_{pt}) in high frequency and the right semicircle refers to the charge transfer resistance at FTO/TiO_2/dye-electrolyte interface (R_{tr}) in low frequency. It is obvious from data also presented in Table 4 that the lower resistance to the electrode-electrolyte interface is calculated for 10 μL AcOH case in absolute agreement with J-V electrical results. However, similar results for all electrodes were obtained for charge transfer at the FTO/TiO_2/dye-electrolyte interface according to Bode plots illustrated in Figure 11b. Charge transfer is related to the frequency peak position (f_{max}) to the plot. Since the charge carrier lifetime is inversely proportional to fmax, the electron lifetime (τ_e) estimated from the expression $\tau_e=1/2\pi f_{max}$ indicates that all electrodes have long charge carrier lifetimes from 25-26 msec.

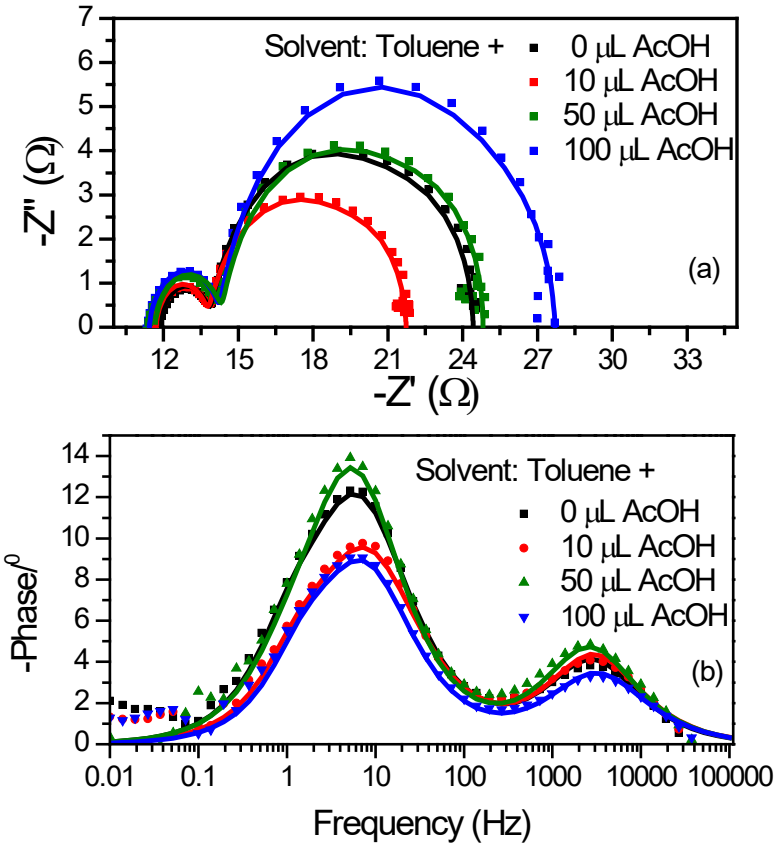

Figure 11. (a) Impedance spectra and (b) Bode phase plots of dye-sensitized solar cells with **BTZA-II** from toluene solutions with various amounts of AcOH measured at open circuit voltage at 1 sun illumination.

CONCLUSIONS

The photophysical and solar cell properties of an organic sensitizer incorporating triphenylamine electron donor and benzothiazole acceptor have been studied. The dye molecules in solutions are found in neutral and anionic form and the photophysics as well as solar cells efficiency are largely dependent on the equilibrium between these two species. Our goal was to investigate and differentiate the photophysical properties of the neutral and anionic form of the dye, to determine the effect of solvent acidity on the solar cell performance and finally to increase the solar cell efficiency through a simple and efficient method. Initially, dye solutions with various solute concentrations, as well as with various amounts of a strong base or acetic acid have been studied, shifting thus the equilibrium systematically towards the neutral (COOH) or the anionic (COO^-) dye form. Upon increasing the concentration, the amount of neutral species increase. In toluene, the neutral and anionic species have a lifetime of 1.8 and 1.1 ns, respectively and both contribute to the emission. However, in acetonitrile, the emission is governed by only the anionic form having a lifetime of 2.0 ns, while the neutral ones are highly quenched with a lifetime of 0.5 ns. These results are corroborated by those obtained when the base DBU or acetic acid were added to the solution to produce anions or neutral species, respectively. The above results clearly indicate that the thorough understanding of the photophysics of organic sensitizers in solutions is more complex and one should be very careful to separate the contributions of anions and neutral species which are solvent- and concentration-dependent and differ in spectral properties. Finally, a remarkable increase of the solar cell efficiency was achieved after addition of a small, appropriate amount of acetic acid to the initial dye solution. The photoelectric conversion efficiency of **BTZA-II** dye increased from initial η=3.1% to η=4.9%, thus by 58%. We believe that this simple yet efficient method for increasing the solar cell performance will be applied in other organic as well as metal-based sensitizers comprising a carboxylic or phosphoric acid group.

ACKNOWLEDGEMENTS

Prof. M. Fakis gratefully acknowledges the financial support by Grant E.028 from the Research Committee of the University of Patras (Programme K. Karatheodori). The synthetic and computational work has been supported by the Ministry of Education, Science, Research and Sport of the Slovak Republic and by the Slovak Research and Development Agency under contracts 1/0712/18 (VEGA) and APVV-17-0324, respectively. Dr. P. Hrobárik also acknowledges funding from the European Union's Horizon 2020 research and innovation programme under the Marie Skłodowska-Curie Grant Agreement No. 752285.

ASSOCIATED CONTENT

Supporting Information. Supplemental data including details on the photophysical properties, stationary spectra, time resolved dynamics and additional solar cell characteristics. This information is available free of charge via the Internet at http://pubs.acs.org.

AUTHOR INFORMATION

*Email: fakis@upatras.gr

**Email: peter.hrobarik@uniba.sk

REFERENCES

1. Mishra, A.; Fischer, M. K. R.; Bäuerle, P. Metal-Free Organic Dyes for Dye-Sensitized Solar Cells: From Structure: Property Relationships to Design Rules. *Angew. Chem. Int. Ed.* **2009,** *48*, 2474-2499.
2. Yen, Y.-S.; Chou, H.-H.; Chen, Y.-C.; Hsu, C.-Y.; Lin, J. T. Recent Developments in Molecule-Based Organic Materials for Dye-Sensitized Solar Cells. *J. Mater. Chem.* **2012**, *22*, 8734-8747.
3. Zeng, W.; Cao, Y.; Bai, Y.; Wang, Y.; Shi, Y.; Zhang, M.; Wang, F.; Pan, C.; Wang, P. Efficient Dye-Sensitized Solar Cells with an Organic Photosensitizer Featuring Orderly Conjugated Ethylenedioxythiophene and Dithienosilole Blocks. *Chem. Mater.* **2010**, *22*, 1915-1925.
4. Tsao, H. N.; Burschka, J.; Yi, C.; Kessler, F.; Nazeeruddin, M. K.; Grätzel, M. Influence of the Interfacial Charge-Transfer Resistance at the Counter Electrode in Dye-Sensitized Solar Cells Employing Cobalt Redox Shuttles. *Energ. Environ. Sci.* **2011**, *4*, 4921-4924.
5. Zhang, M.; Wang, Y.; Xu, M.; Ma, W.; Li, R.; Wang, P. Design of High-Efficiency Organic Dyes for Titania Solar Cells Based on the Chromophoric Core of Cyclopentadithiophene-Benzothiadiazole. *Energ. Environ. Sci.* **2013**, *6*, 2944-2949.
6. Hagfeldt, A.; Boschloo, G.; Sun, L.; Kloo, L.; Pettersson, H. Dye-Sensitized Solar Cells. *Chem. Rev.* **2010**, *110*, 6595-6663.
7. Srinivasan, V.; Panneer, M.; Jaccob, M.; Pavithra, N.; Anandan, S.; Kathiravan, A. A Diminutive Modification in Arylamine Electron Donors: Synthesis, Photophysics and Solvatochromic Analysis-Towards the Understanding of Dye Sensitized Solar Cell Performances. *Phys. Chem. Chem. Phys.* **2015**, *17*, 28647-28657.

8. Liang, M.; Xu, W.; Cai, F.; Chen, P.; Peng, B.; Chen, J.; Li, Z. New Triphenylamine-Based Organic Dyes for Efficient Dye-Sensitized Solar Cells. *J. Phys. Chem. C* **2007**, *111*, 4465-4472.
9. Jiang, S.; Fan, S.; Lu, X.; Zhou, G.; Wang, Z. S. Double D-π-A Branched Organic Dye Isomers for Dye-Sensitized Solar Cells. *J. Mater.Chem. A* **2014**, *2*, 17153–17164.
10. Li, Y.; Wang, J.; Yuan, Y.; Zhang, M.; Dong, X.; Wang, P. Correlating Excited State and Charge Carrier Dynamics with Photovoltaic Parameters of Perylene Dye Sensitized Solar Cells: Influences of an Alkylated Carbazole Ancillary Electron-Donor. *Phys. Chem. Chem. Phys.* **2017**, *19*, 2549-2556.
11. Arbouch, I.; Cornil, D.; Karzazi, Y.; Hammouti, B.; Lazzaroni, R.; Cornil, J. Influence of the Nature of the Anchoring Group on Electron Injection Processes at Dye-Titania Interfaces. *Phys. Chem. Chem. Phys* **2017**, *19*, 29389-29401.
12. Roiati, V.; Giannuzzi, R.; Lerario, G.; Marco, L. De; Agosta, R.; Iacobellis, R.; Grisorio, R.; Suranna, G. P.; Listorti, A.; Gigli, G. Beneficial Role of a Bulky Donor Moiety in π-Extended Organic Dyes for Mesoscopic TiO_2 Sensitized Solar Cells. *J. Phys. Chem. C* **2015**, *119*, 6956-6965.
13. Yao, Z.; Zhang, M.; Wu, H.; Yang, L.; Li, R.; Wang, P. Donor/Acceptor Indenoperylene Dye for Highly Efficient Organic Dye-Sensitized Solar Cells. *J. Am. Chem. Soc.* **2015**, *137*, 3799-3802.
14. Castellucci, E.; Monini, M.; Bessi, M.; Iagatti, A.; Bussotti, L.; Sinicropi, A.; Calamante, M.; Zani, L.; Basosi, R.; Reginato, G.; et al. Photoinduced Excitation and Charge Transfer Processes of Organic Dyes with Siloxane Anchoring Groups: A Combined Spectroscopic and Computational Study. *Phys. Chem. Chem. Phys.* **2017**, *19*, 15310-15323.
15. Chiu, K. Y.; Ha Tran, T. T.; Chang, S. H.; Yang, T. F.; Su, Y. O. A New Series of Azobenzene-Bridged Metal-Free Organic Dyes and Application on DSSC. *Dyes Pigm*. **2017**, 146, 512-519.
16. Tingare, Y. S.; Vinh, N. S.; Chou, H. H.; Liu, Y. C.; Long, Y. S.; Wu, T. C.; Wei, T. C.; Yeh, C. Y. New Acetylene-Bridged 9,10-Conjugated Anthracene Sensitizers: Application in Outdoor and Indoor Dye-Sensitized Solar Cells. *Adv. Energy Mater.* **2017**, *7*, 1700032.
17. Alagumalai, A.; Munavvar, M. F.; Vellimalai, P.; Sil, M. C.; Nithyanandhan, J. Effect of Out-of-Plane Alkyl Group's Position in Dye-Sensitized Solar Cell Efficiency: A Structure-Property Relationship Utilizing Indoline-Based Unsymmetrical Squaraine Dyes. *ACS Appl. Mater. Interfaces* **2016**, *8*, 35353–35367.

18. Bobe, S. R.; Gupta, A.; Rananaware, A.; Bilic, A.; Xiang, W.; Li, J. L.; Bhosale, S. V.; Bhosale, S. V.; Evans, R. A. Insertion of a Naphthalenediimide Unit in a Metal-Free Donor–acceptor Organic Sensitizer for Efficiency Enhancement of a Dye-Sensitized Solar Cell. *Dyes Pigm.* **2016**, *134*, 83-90.
19. Knyazeva, E. A.; Wu, W.; Chmovzh, T. N.; Robertson, N.; Woollins, J. D.; Rakitin, O. A. Dye-Sensitized Solar Cells: Investigation of D-A-π-A Organic Sensitizers Based on [1,2,5]Selenadiazolo[3,4-c]Pyridine. *Sol. Ener.* **2017**, *144*, 134-143.
20. Eom, Y. K.; Choi, I. T.; Kang, S. H.; Lee, J.; Kim, J.; Ju, M. J.; Kim, H. K. Thieno[3,2-b][1]Benzothiophene Derivative as a New π-Bridge Unit in D-π-A Structural Organic Sensitizers with over 10.47% Efficiency for Dye-Sensitized Solar Cells. *Adv. Energy Mater.* **2015**, *5*, 1500300.
21. Zhang, M.-D.; Xie, H.-X.; Ju, X.-H.; Qin, L.; Yang, Q.-X.; Zheng, H.-G.; Zhou, X.-F. D-D-π-A Organic Dyes Containing 4,4'-Di(2-Thienyl)Triphenylamine Moiety for Efficient Dye-Sensitized Solar Cells. *Phys. Chem. Chem. Phys.* **2013**, *15*, 634-641.
22. Hosseinzadeh, B.; Beni, A. S.; Azari, M.; Zarandi, M.; Karami, M. Novel D-π-A Type Triphenylamine Based Chromogens for DSSC: Design, Synthesis and Performance Studies. *New J. Chem.* **2016**, *40*, 8371-8381.
23. Zhao, J.; Yang, X.; Cheng, M.; Li, S.; Sun, L. Molecular Design and Performance of Hydroxylpyridium Sensitizers for Dye-Sensitized Solar Cells. *ACS Appl. Mater. Interfaces* **2013**, *5*, 5227-5231.
24. Zhou, N.; Prabakaran, K.; Lee, B.; Chang, S. H.; Harutyunyan, B.; Guo, P.; Butler, M. R.; Timalsina, A.; Bedzyk, M. J.; Ratner, M. A.; et al. Metal-Free Tetrathienoacene Sensitizers for High-Performance Dye-Sensitized Solar Cells. *J. Am. Chem. Soc.* **2015**, *137*, 4414-4423.
25. Khamrang, T.; Velusamy, M.; Jaccob, M.; Ramesh, M.; Kathiresan, M.; Kathiravan, A. A Combined Experimental and Computational Investigation on Pyrene Based D-π-A Dyes. *Phys. Chem. Chem. Phys.* **2018**, *20*, 6264-6273.
26. Tan, L. L.; Huang, J. F.; Shen, Y.; Xiao, L. M.; Liu, J. M.; Kuang, D. Bin; Su, C. Y. Highly Efficient and Stable Organic Sensitizers with Duplex Starburst Triphenylamine and Carbazole Donors for Liquid and Quasi-Solid-State Dye-Sensitized Solar Cells. *J. Mater.Chem. A* **2014**, *2*, 8988-8994.
27. P. Gao, H. N. Tsao, C. Yi, M. Grätzel and M. K. Nazeeruddin, Adv. Energy Mater., 2014, 4, 1301485. Gao, P.; Tsao, H. N.; Yi, C.; Grätzel, M.; Nazeeruddin, M. K. Extended π-Bridge in Organic Dye-Sensitized Solar Cells: The Longer, the Better? *Adv. Energy Mater.* **2014**, *4*, 1301485.

28. Wang, Y.; Dong, L.; Zheng, Z.; Li, X.; Xiong, R.; Hua, J.; Hu, A. Enediyne as π Linker in D-π-A Dyes for Dye-Sensitized Solar Cells. *RSC Adv.* **2016**, *6*, 12124-12130.
29. Oum, K.; Lohse, P. W.; Klein, J. R.; Flender, O.; Scholz, M.; Hagfeldt, A.; Boschloo, G.; Lenzer, T. Photoinduced Ultrafast Dynamics of the Triphenylamine-Based Organic Sensitizer D35 on TiO_2, ZrO_2 and in Acetonitrile. *Phys. Chem. Chem. Phys.* **2013**, *15*, 3906-3916.
30. Tan, C.-J.; Yang, C.-S.; Sheng, Y.-C.; Amini, H. W.; Gavin Tsai H.-H. Spacer Effects of Donor-π Spacer-Acceptor Sensitizers on Photophysical Properties in Dye-Sensitized Solar Cells. *J. Phys. Chem. C* **120**, *38*, 21272-21284.
31. Pei, K.; Wu, Y.; Wu, W.; Zhang, Q.; Chen, B.; Tian, H.; Zhu, W. Constructing Organic D-A-π-A-Featured Sensitizers with a Quinoxaline Unit for High-Efficiency Solar Cells: The Effect of an Auxiliary Acceptor on the Absorption and the Energy Level Alignment. *Chem. Eur. J.* **2012**, *18*, 8190-8200.
32. Bairu, S. G.; Mghanga, E.; Hasan, J.; Kola, S.; Rao, V. J.; Bhanuprakash, K.; Giribabu, L.; Wiederrecht, G. P.; Da Silva, R.; Rego, L. G. C.; et al. Ultrafast Interfacial Charge-Transfer Dynamics in a Donor-π-Acceptor Chromophore Sensitized TiO_2 Nanocomposite. *J. Phys. Chem. C* **2013**, *117*, 4824-4835.
33. Kathiravan, A.; Srinivasan, V.; Khamrang, T.; Velusamy, M.; Jaccob, M.; Pavithra, N.; Anandan, S.; Velappan, K. Pyrene Based D-π-A Architectures: Synthesis, Density Functional Theory, Photophysics and Electron Transfer Dynamics. *Phys. Chem. Chem. Phys.* **2017**, *19*, 3125-3135.
34. Fakis, M.; Hrobárik, P.; Yushchenko, O.; Sigmundová, I.; Koch, M.; Rosspeintner, A.; Stathatos, E.; Vauthey, E. Excited State and Injection Dynamics of Triphenylamine Sensitizers Containing a Benzothiazole Electron-Accepting Group on TiO_2 and Al_2O_3 Thin Films. *J. Phys. Chem. C* **2014**, *118*, 28509-28519.
35. Fakis, M.; Stathatos, E.; Tsigaridas, G.; Giannetas, V.; Persephonis, P. Femtosecond Decay and Electron Transfer Dynamics of the Organic Sensitizer D149 and Photovoltaic Performance in Quasi-Solid-State Dye-Sensitized Solar Cells. *J. Phys. Chem. C* **2011**, *115*, 13429-13437.
36. Rohwer, E.; Minda, I.; Tauscher, G.; Richter, C.; Miura, H.; Schlettwein, D.; Schwoerer, H. Ultrafast Charge-Transfer Reactions of Indoline Dyes with Anchoring Alkyl Chains of Varying Length in Mesoporous ZnO Solar Cells. *ChemPhysChem* **2015**, *16*, 943-948.

37. Li, Y.; Lu, P.; Yan, X.; Jin, L.; Peng, Z. Non-Aggregated Hyperbranched Phthalocyanines: Single Molecular Nanostructures for Efficient Semi-Opaque Photovoltaics. *RSC Adv.* **2013**, *3*, 545–558.
38. Pijpers, J. J. H.; Ulbricht, R.; Derossi, S.; Reek, J. N. H.; Bonn, M. Picosecond Electron Injection Dynamics in Dye-Sensitized Oxides in the Presence of Electrolyte. *J. Phys. Chem. C* **2011**, *115*, 2578–2584.
39. Chang, Y. C.; Wu, H. P.; Reddy, N. M.; Lee, H. W.; Lu, H. P.; Yeh, C. Y.; Diau, E. W. G. The Influence of Electron Injection and Charge Recombination Kinetics on the Performance of Porphyrin-Sensitized Solar Cells: Effects of the 4-Tert-Butylpyridine Additive. *Phys. Chem. Chem. Phys.* **2013**, *15*, 4651-4655.
40. Ziółek, M.; Tacchini, I.; Martínez, M. T.; Yang, X.; Sun, L.; Douhal, A. A Photo-Induced Electron Transfer Study of an Organic Dye Anchored on the Surfaces of TiO_2 Nanotubes and Nanoparticles. *Phys. Chem. Chem. Phys.* **2011**, *13*, 4032-4044.
41. Teuscher, J.; Décoppet, J. D.; Punzi, A.; Zakeeruddin, S. M.; Moser, J. E.; Grätzel, M. Photoinduced Interfacial Electron Injection Dynamics in Dye-Sensitized Solar Cells under Photovoltaic Operating Conditions. *J. Phys. Chem. Lett.* **2012**, *3*, 3786-3790.
42. Wang, L.; Wang, H. Y.; Fang, H. H.; Weng, H.; Yang, Z. Y.; Gao, B. R.; Chen, Q. D.; Han, W.; Sun, H. B. Universal Electron Injection Dynamics at Nanointerfaces in Dye-Sensitized Solar Cells. *Adv. Funct. Mater.* **2012**, *22*, 2783-2791.
43. Zhang, J.; Yao, Z.; Cai, Y.; Yang, L.; Xu, M.; Li, R.; Zhang, M.; Dong, X.; Wang, P. Conjugated Linker Correlated Energetics and Kinetics in Dithienopyrrole Dye-Sensitized Solar Cells. *Energ. Environ. Sci.* **2013**, *6*, 1604-1614.
44. Oum, K.; Lohse, P. W.; Flender, O.; Klein, J. R.; Scholz, M.; Lenzer, T.; Du, J.; Oekermann, T. Ultrafast Dynamics of the Indoline Dye D149 on Electrodeposited ZnO and Sintered ZrO_2 and TiO_2 Thin Films. *Phys. Chem. Chem. Phys.* **2012**, *14*, 15429-15437.
45. Ziółek, M.; Yang, X.; Sun, L.; Douhal, A. Interrogating the Ultrafast Dynamics of an Efficient Dye for Sunlight Conversion. *Phys. Chem. Chem. Phys.* **2010**, *12*, 8099-8108.
46. El-Zohry, A. M.; Zietz, B. Concentration and Solvent Effects on the Excited State Dynamics of the Solar Cell Dye D149: The Special Role of Protons. *J. Phys. Chem. C* **2013**, *117*, 6544-6553.
47. Dryza, V.; Bieske, E. J. Does the Triphenylamine-Based D35 Dye Sensitizer Form Aggregates on Metal-Oxide Surfaces? *J. Photochem. Photobiol. A* **2015**, *302*, 35-41.
48. Dryza, V.; Nguyen, J. L.; Kwon, T. H.; Wong, W. W. H.; Holmes, A. B.; Bieske, E. J. Photophysics and Aggregation Effects of a Triphenylamine-Based Dye Sensitizer on Metal-

Oxide Nanoparticles Suspended in an Ion Trap. *Phys. Chem. Chem. Phys.* **2013**, *15*, 20326-20332.

49. Debnath, T.; Maity, P.; Lobo, H.; Singh, B.; Shankarling, G. S.; Ghosh, H. N. Extensive Reduction in Back Electron Transfer in Twisted Intramolecular Charge-Transfer (TICT) Coumarin-Dye-Sensitized TiO_2 Nanoparticles/Film: A Femtosecond Transient Absorption Study. *Chem. Eur. J.* **2014**, *20*, 3510-3519.
50. Chen, K. F.; Chang, C. W.; Lin, J. L.; Hsu, Y. C.; Yeh, M. C. P.; Hsu, C. P.; Sun, S. S. Photophysical Studies of Dipolar Organic Dyes That Feature a 1,3-Cyclohexadiene Conjugated Linkage: The Implication of a Twisted Intramolecular Charge-Transfer State on the Efficiency of Dye-Sensitized Solar Cells. *Chem. Eur. J.* **2010**, *16*, 12873-12882.
51. Verma, S.; Ghosh, H. N. Tuning Interfacial Charge Separation by Molecular Twist: A New Insight into Coumarin-Sensitized TiO_2 Films. *J. Phys. Chem. C* **2014**, *118*, 10661-10669.
52. Sobuś, J.; Burdziński, G.; Karolczak, J.; Idígoras, J.; Anta, J. A.; Ziółek, M. Comparison of TiO_2 and ZnO Solar Cells Sensitized with an Indoline Dye: Time-Resolved Laser Spectroscopy Studies of Partial Charge Separation Processes. *Langmuir*, **2014**, *30*, 2505-2512.
53. Scholz, M.; Flender, O.; Boschloo, G.; Oum K.; Lenzer, T. Ultrafast Electron and Hole Transfer Dynamics of a Solar Cell Dye Containing Hole Acceptors on Mesoporous TiO_2 and Al_2O_3. *Phys. Chem. Chem. Phys*. **2017**, *19*, 7158-7166.
54. Ozawa, H.; Awa, M.; Ono T.; Arakawa, H. Effects of Dye-Adsorption Solvent on the Performances of the Dye-Sensitized Solar Cells Based on Black Dye. *Chem. Asian J.* **2012**, *7*, 156-162.
55. Tian, H.; Yang, X.; Chen, R.; Zhang, R.; Hagfeldt A.; Sun, L. Effect of Different Dye Baths and Dye-Structures on the Performance of Dye-Sensitized Solar Cells Based on Triphenylamine Dyes. *J. Phys. Chem. C* **2008**, *112*, 11023-11033.
56. Marotta, G.; Lobello, M. G.; Anselmi, C.; Consiglio, G. B.; Calamante, M.; Mordini, A.; Pastore M.; De Angelis, F. An Integrated Experimental and Theoretical Approach to the Spectroscopy of Organic-Dye-Sensitized TiO_2 Heterointerfaces: Disentangling the Effects of Aggregation, Solvation, and Surface Protonation. *ChemPhysChem*, **2014**, *15*, 1116–1125.
57. Jeon, B. C.; Kim, M. S.; Cho, M. J.; Choi, D. H.; Ahn K. S.; Kim, J. H. Effect of Solvent on Dye-Adsorption Process and Photovoltaic Properties of Dendritic Organic Dye on TiO_2 Electrode of Dye-Sensitized Solar Cells. *Synth. Met*. **2014**, *188*, 130–135.

58. Droseros, N.; Seintis, K.; Fakis, M.; Gardelis S.; Nassiopoulou, A. G. Steady State and Time Resolved Photoluminescence Properties of $CuInS_2$/ZnS Quantum Dots in Solutions and in Solid Films. *J. Lumin*. **2015**, *167*, 333-338.
59. Sygkridou, D.; Rapsomanikis A.; Stathatos, E. Functional Transparent Quasi-Solid State Dye-Sensitized Solar Cells made with Different Oligomer Organic/Inorganic Hybrid Electrolytes. *Sol. Energy Mater. Sol. Cells* **2017**, *159*, 600-607.
60. Frisch, M. J.; Trucks, G. W.; Schlegel, H. B.; Scuseria, G.; Robb, M. A.; Cheeseman, J. R.; Scalmani, G.; Barone, V.; Mennucci, B.; Petersson, G. A. et al. Gaussian 09, revision D.01; Gaussian, Inc.: Wallingford, CT, **2009**.
61. Yanai, T.; Tew D. P.; Handy, N. C. A New Hybrid Exchange–Correlation Functional using the Coulomb-Attenuating Method (CAM-B3LYP). *Chem. Phys. Lett*. **2004**, *393*, 51−57.
62. Tomasi, J.; Mennucci, B.; Cammi, R. Quantum Mechanical Continuum Solvation Models. *Chem. Rev*. **2005**, *105*, 2999−3093.
63. Taft, R. W.; Kamlet, M. J. The Solvatochromic Comparison Method. 2. The Alpha.-Scale of Solvent Hydrogen-Bond Donor (HBD) Acidities. *J. Am. Chem. Soc.* **1976**, *98*, 2886–2894.
64. Lippert, E.; *Z.* Dipolmoment und Elektronenstruktur von Angeregten Molekülen. *Naturforsch. A* **1955**, *10*, 541-545.
65. Mataga, N.; Kaifu Y.; Koizumi, M. The Solvent Effect on Fluorescence Spectrum, Change of Solute-Solvent Interaction during the Lifetime of Excited Solute Molecule. *Bull. Chem. Soc. Jpn*. **1955**, *28*, 690-691.
66. Lacowicz, J. R. Principles of Fluorescence Spectroscopy, Springer, **2006**.
67. Bang, H. G.; Chung, J. K.; Jung R. Y.; Park, S. Y. Effect of Acetic Acid in TiO_2 Paste on the Performance of Dye-Sensitized Solar Cells. *Ceram. Int*. **2012**, *38*, S511–S515.
68. Ito, S.; Chen, P.; Comte, P.; Nazeeruddin, M. K.; Liska, P.; Péchy P.; Grätzel, M. Fabrication of Screen-Printing Pastes from TiO_2 Powders for Dye-Sensitised Solar Cells. *Prog. Photovoltaics*. **2007**, *15*, 603–612.
69. Tae, E. L.; Lee, S. H.; Lee, J. K.; Yoo, S. S.; Kang, E. J.; Yoon, K. B. A Strategy To Increase the Efficiency of the Dye-Sensitized TiO_2 Solar Cells Operated by Photoexcitation of Dye-to-TiO_2 Charge-Transfer Bands *J. Phys. Chem. B*, **2005**, *109*, 22513-22522.
70. Suresh, T.; Chitumalla, R. K.; Hai, N. T.; Jang, J.; Lee T. J.; Kim J. H. Impact of neutral and anion anchoring groups on the photovoltaic performance of triphenylamine sensitizers for dye-sensitized solar cells. *RSC Adv.* **2016**, 6, 26559-26567.

71. Nagarajan, B.; Kushwaha, S.; Elumalai, R.; Mandal, S.; Ramanujam K.; Raghavachari, D. Novel Ethynyl-Pyrene Substituted Phenothiazine Based Metal Free Organic Dyes in DSSC with 12% Conversion Efficiency. *J. Mater. Chem. A*, **2017**, *5*, 10289-10300.
72. Yang, G.; Tang, Y.; Li, X.; Agren H.; Xie, Y. Efficient Solar Cells Based on Porphyrin Dyes with Flexible Chains Attached to the Auxiliary Benzothiadiazole Acceptor: Suppression of Dye Aggregation and the Effect of Distortion. *ACS Appl. Mater. Interfaces* **2017**, *9*, 36875–36885.
73. Jungsuttiwong, S.; Sirithip, K.; Prachumrak, N.; Tarsang, R.; Sudyoadsuk, T.; Namuangruk, S.; Kungwan, N.; Promarak, V.; Keawin, T. Significant Enhancement in the Performance of Porphyrin for Dye-Sensitized Solar Cells: Aggregation Control using Chenodeoxycholic Acid. *New J. Chem*. **2017**, *41*, 7081-7091.
74. Huang, Z. S.; Feng, H. L.; Zang, X. F.; Iqbal, Z.; Zeng, H.; Kuang, D. B.; Wang, L.; Meier H.; Cao, D. Dithienopyrrolobenzothiadiazole-Based Organic Dyes for Efficient Dye-Sensitized Solar Cells. *J. Mater. Chem. A* **2014**, *2*, 15365-15376.
75. Lin, R. Y. Y.; Wu, F. L.; Chang, C. H.; Chou, H. H.; Chuang, T. M.; Chu, T. C.; Hsu, C. Y.; Chen, P. W.; Ho, K. C.; Lo Y. H. et al. Y-Shaped Metal-Free D–π–$(A)_2$ Sensitizers for High-Performance Dye-Sensitized Solar Cells. *J. Mater. Chem. A* **2014**, *2*, 3092-3101.
76. Salvatori, P.; Marotta, G.; Cinti, A.; Anselmi, C.; Mosconi E.; De Angelis, F. Supramolecular Interactions of Chenodeoxycholic Acid Increase the Efficiency of Dye-Sensitized Solar Cells Based on a Cobalt Electrolyte. *J. Phys. Chem. C* **2013**, *117*, 3874–3887.
77. Dori, M.; Seintis, K.; Stathatos, E.; Tsigaridas, G.; Lin, T. Y.; Lin, J. T.; Fakis, M.; Giannetas V.; Persephonis, P. Electron Injection Studies in TiO_2 Nanocrystalline Films Sensitized with Fluorene Dyes and Photovoltaic Characterization. The Effect of Co-Adsorption of a Bile Acid Derivative. *Chem. Phys. Lett*. **2013**, *563*, 63–69.

TOC Graphic

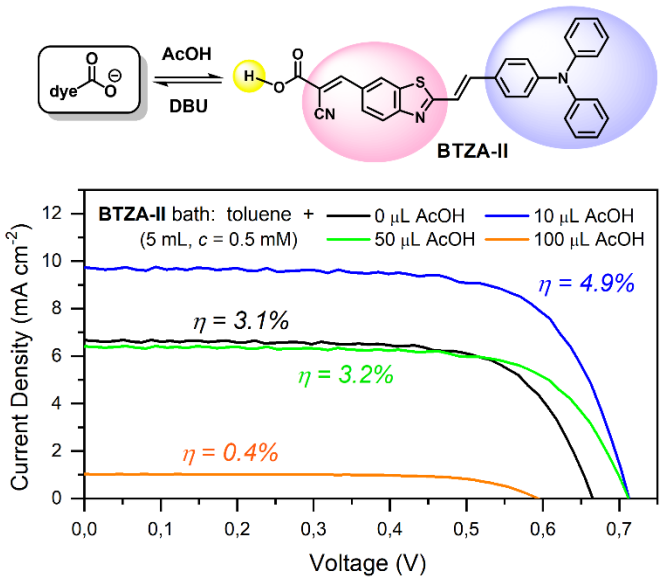
AcOH
DBU
dye
CN
S
N
BTZA-II
BTZA-II bath: toluene +
(5 mL, c = 0.5 mM)
0 μL AcOH
10 μL AcOH
50 μL AcOH
100 μL AcOH
η = 4.9%
η = 3.1%
η = 3.2%
η = 0.4%
Current Density (mA cm-2)
Voltage (V)
0
2
4
6
8
10
12
0,0
0,1
0,2
0,3
0,4
0,5
0,6
0,7